

Intestinal injury alters tissue distribution and toxicity of ZnO nanoparticles in mice

Li-Jing Du^{a,1}, Kun Xiang^{a,1,2}, Jia-Hui Liu^b, Zheng-Mei Song^a, Yuanfang Liu^{a,c}, Aoneng Cao^a, Haifang Wang^{a,*}

^a Institute of Nanochemistry and Nanobiology, Shanghai University, Shanghai 200444, China

^b Beijing Key Laboratory of Bioprocess, College of Life Science and Technology, Beijing University of Chemical Technology, Beijing 100029, China

^c Beijing National Laboratory for Molecular Sciences, College of Chemistry and Molecular Engineering, Peking University, Beijing 100871, China



ARTICLE INFO

Keywords:

Zinc oxide nanoparticle
Biodistribution
Nanotoxicity
Intestinal injury
Inflammatory bowel disease
Trace element

ABSTRACT

The fast growing applications of ZnO nanoparticles (NPs) in food sector and other fields enhance the exposure possibility of human beings to ZnO NPs including via oral administration route. Although the oral toxicity of ZnO NPs has been studied, most of the research was performed on the normal animal models. Therefore, the understanding of the biological consequence of ZnO NPs on the population with diseases, especially gastrointestinal disease, is extremely limited. In this study, a mice model of inflammatory bowel disease (IBD) induced by indomethacin has been developed to comprehensively investigated the bioeffects of ZnO NPs on the specific population. The effect of the intestinal inflammation/injury on the distribution and toxicity of orally administered ZnO NPs (nZnO, 20 nm × 100 nm and mZnO, ~200 nm) in mice were analyzed. The results showed that there was a difference in the distribution of Zn and the essential trace elements (Fe and Cu) between the IBD mice and the normal mice. We also observed an obvious size effect. Higher hepatic Zn was detected in the IBD mice post-exposure to ZnO NPs, especially bigger ZnO NPs. In addition, the histopathological examination of main organs and biological parameters analysis showed that ZnO NPs caused slight toxicity to the liver and kidneys in the IBD mice. Our findings highlight the importance of the health status of animals on the bioeffects of nanomaterials.

1. Introduction

Accumulated consumer products containing engineered nanomaterials have been launched to the market with the development of nanotechnology (Vance et al., 2015). For instance, ZnO NPs are used for nutritional purposes in food based on the enhanced gastrointestinal Zn uptake, and they have been added into food packaging materials or coated onto dental implants due to the excellent antibacterial ability (Akbar and Anal, 2014; Bouwmeester et al., 2009; Espitia et al., 2012; Llorens et al., 2012; Memarzadeh et al., 2015). Additionally, ZnO NPs have also become the important ingredient of sunscreen products (Contado, 2015; Gulson et al., 2015; Osmond and Mccall, 2010). Furthermore, ZnO NPs are involved in many biomedical applications, such as drug delivery, tissue regeneration, bioimaging and disease therapy (Umrani and Paknikar, 2014; Zhang et al., 2011; Zhu et al., 2016). Therefore, people are inevitably exposed to ZnO NPs, especially intake orally through the consuming food and other products.

The biodistribution and toxicity of ZnO NPs after the oral administration have been studied. It has been found that only a small amount of ZnO NPs could enter the circulatory system and accumulate in some organs, like liver (Wang et al., 2013a); while the great majority of orally administrated ZnO NPs could not be absorbed, they are mostly excreted via feces (Liu et al., 2017). As for the toxicity of ZnO NPs, organ damages of the liver and other organs have been reported. Li and colleagues observed slightly transient liver histopathological lesions in the mice following exposure to 2.5 g ZnO NPs/kg body weight (b.w.) (Li et al., 2012). Moreover, ZnO NPs have also been found to increase the blood viscosity and induce pathological damage in the stomach, liver, heart and spleen (Wang et al., 2008). The liver damage was normally attributed to the oxidative stress induced by Zn accumulation, which would end up with DNA damage and cell apoptosis. Particularly, the toxicity of ZnO NPs could be varied based on the physical property and dosage (Cho et al., 2013; Park et al., 2014).

Age and health status-related difference in response to

* Corresponding author.

E-mail address: hwang@shu.edu.cn (H. Wang).

¹ These authors contributed equally to this work.

² Present address: Department of Biomedical Engineering, Duke University, Durham, NC 27708, USA.

nanomaterials have been demonstrated by several groups. For example, Wang et al. reported that TiO_2 NPs presented different toxic effects on young and adult rats (Wang et al., 2013b). The liver edema, heart injuries and non-allergic mast cell activation in stomach tissues were found in young rats, while only slight injury in the liver and kidney and decreased intestinal permeability and molybdenum contents were found in adult rats. Swietlicki et al. found that the deposited dose rate of diesel combustion particles increased with increasing severity of the chronic obstructive pulmonary disease, however, the deposition probability of the combustion particles less than 100 nm was decreased in chronic obstructive pulmonary disease patients (Swietlicki et al., 2012). Recently, Jia et al. (2017) reported that ZnO NPs enhanced the deposition of Pb in all major organs in the overweight mice compared with that in the normal mice after orally administered ZnO NPs and lead acetate at tolerable dose. ZnO NPs at certain concentrations also were found to show cardio-protective role in diabetic rats and induce cardiac damage in healthy rats (Asri-Rezaei et al., 2017). It is well known that the physiology of the gastrointestinal tract changes the absorption of various substances, and then even induces the adverse health effect (Hakata et al., 2005). Nanomaterials should be no exception (Des Rieux et al., 2006).

However, the aforementioned distribution and toxicity studies about ZnO NPs were performed on the normal animal models. It would be necessary to investigate how the altered health status of gastrointestinal tract (like intestinal injury or inflammatory bowel disease (IBD)) would affect the behaviors of ZnO NPs *in vivo*. Thus, in this study, the indomethacin induced IBD mouse model was developed to evaluate the behaviors of orally administrated ZnO NPs. The results suggested that the alteration of intestinal health status would affect the distribution and bioeffect of ZnO NPs.

2. Materials and methods

2.1. Nanoparticles and reagents

ZnO NPs, nZnO (rod shape, $20\text{ nm} \times 100\text{ nm}$) and mZnO (cubic shape, $\sim 200\text{ nm}$), were purchased from Pengyuan Chemical Co., Ltd. (Guangzhou, China) and Haihua Group Co., Ltd. (Shandong, China), respectively. Indomethacin and hexadecyltrimethyl ammonium bromide were obtained from Sigma-Aldrich (USA), and dihydrochloride O-dianisidine from Alfa Aesar (USA). Deionized water ($18.2\text{ M}\Omega\text{-cm}$; Milli-Q system, Millipore Co., USA) was used to prepare all the solutions and suspensions.

2.2. Characterization of ZnO NPs

The morphology and size of ZnO NPs were determined by transmission electron microscopy (TEM, JEM-200CX, JEOL, Japan) operating at 120 kV. TEM samples were prepared by suspending ZnO particles in deionized water, dropping onto polycarbon-coated copper grids and drying at room temperature overnight. The crystalline phase of ZnO NPs was characterized by X-ray diffraction (XRD, Rigaku Co., Tokyo, Japan). X-ray fluorescence (XRF, S4-Explorer, Bruker, Germany) was adopted to analyze the purity. The suspensions of ZnO particles were prepared by dispersing in deionized water under sonication (40 kHz, 50 W) just prior to the administration. The hydrodynamic size and zeta-potential of ZnO NPs in water were measured with a Nanosizer (DLS; Nano ZS90, Malvern, Mordern, UK).

2.3. Dissolution of ZnO NPs in the simulated gastrointestinal digestion juices

To evaluate the dissolution of ZnO NPs in gastrointestinal tract in mice, the previously described *in vitro* digestion simulation method (Peters et al., 2012) was utilized. Before incubation, the juices were heated to 37°C and incubation was carried out in a tabletop orbital shaker (200 rpm, Thermo Scientific, USA) at 37°C . The digestion was

started by shaking the mixture ($\text{pH } 2.0 \pm 0.5$) of 4 ml of gastric juice and 0.12 g of ZnO NPs for 2 h. Subsequently, duodenal juice (4 ml), bile juice (2 ml), and NaHCO_3 solution (0.67 ml) were added. The mixture was adjusted to $\text{pH } 8.0 \pm 0.5$ and shaken for another 2 h. Finally, the mixture was centrifuged ($16,000\text{ rpm} \times 30\text{ min}$, Hitachi CR21GII, Japan) and the supernatant was collected for the Zn content measurement. The measurement was conducted by inductively coupled plasma-mass spectrometry (ICP-MS, ELAN DRC-e, PerkinElmer Co., USA) after the supernatant was digested with HNO_3 (Guaranteed grade, Sinopharm Chemical Reagent Co., Ltd., Shanghai, China) and H_2O_2 (Guaranteed grade, Sinopharm Chemical Reagent Co., Ltd., Shanghai, China) by a microwave digestion system (MARS, CEM, USA). Each datum was obtained from four parallel samples.

2.4. Animals

All animal experiments were performed in compliance with the institutional ethics committee regulations and guidelines on animal welfare (Animal Care and Use Program Guidelines of Shanghai University) with the approval by Shanghai University. The healthy male ICR mice, $25\text{--}27\text{ g}$ (about 8 weeks), were supplied by the Experimental Animal Center, Second Military Medical University (Shanghai, China). The animals were housed in clean polypropylene cages and maintained in an air-conditioned animal house at $23 \pm 2^\circ\text{C}$, $60 \pm 10\%$ relative humidity and 12-h light/dark cycle. The animals were provided with the commercial pellet diet and water *ad libitum*. After one week acclimation, mice were randomly divided into groups: the control, the Indo group (indomethacin treated), the nZnO group, the Indo- nZnO group, the mZnO group and the Indo- mZnO group.

2.5. Developing the IBD mice by indomethacin

The conventional indomethacin induced IBD murine model has been described previously (Bradley et al., 1982; Kawahara et al., 2011; Randhawa et al., 2014). Briefly, mice were given indomethacin (9 mg/kg b.w. , subcutaneous injection) to induce the small intestinal inflammation/injury with 18 h fasting and a 1 h re-feeding cycle. The intestinal inflammation was evaluated by measuring the activity of myeloperoxidase (MPO) of the small intestine, which is an indicator of inflammation (Faith et al., 2008). TEM investigation of small intestine was utilized for further confirmation of intestinal injury through the morphological aspect.

MPO activities of the IBD mice and control were measured following the procedure reported (Bradley et al., 1982; Kawahara et al., 2011). In brief, after the indomethacin treatment for 12 h, the mice were sacrificed and the small intestines were removed, rinsed with cold saline and weighed. The intestine from the normal mice was used as the control. The intestine was homogenized in 4 ml of 50 mM phosphate buffer ($\text{pH } 6.0$), containing 0.5% of hexadecyltrimethylammonium bromide (HTAB) for 45 s at 0°C by a motor-driven homogenizer (AD200L-H, Angni Instruments & Meters Co., Ltd., Shanghai, China). The homogenized samples were subjected to three freeze-thaw cycles, and then centrifuged at $16,000\text{ rpm}$ for 15 min at 4°C for collecting supernatants. The assay mixture contained 0.1 ml of supernatant, 2.9 ml of 50 mM phosphate buffer ($\text{pH } 6.0$), 0.167 mg of dihydrochloride O-dianisidine /ml and 0.0005% (w/v) of H_2O_2 . The absorbance at 450 nm of each sample was recorded along reaction time on a microplate reader (Varioskan Flash, Thermo, USA). The protein content of the sample was estimated by the bicinchoninic acid assay (BCA protein assay kit, Biodee Biological Technology Co., Ltd., Beijing, China). The MPO activity ($\mu\text{mol H}_2\text{O}_2/\text{min mg protein}$) was obtained from the slope of the reaction curve.

For TEM investigation, the segments of small intestine were collected from an IBD mouse at 12 h post indomethacin treatment. The samples were fixed with 2.5% glutaraldehyde in phosphate buffer, and then rinsed by 0.1 M phosphate solution for three times, post-fixed with

1% osmium tetroxide at 4 °C for 2 h. After that, the samples were dehydrated with ethanol and acetone, and double stained with 3% uranyl acetate and lead citrate. Finally, the samples were sectioned using an ultramicrotome (LKB-I, Sweden). TEM images were observed on JEM-1200EX (JEOL, Japan).

2.6. Oral administration of ZnO NPs

After fasting for 18 h and re-feeding for 1 h, mice of the Indo group and the Indo-ZnO groups were given indomethacin (9 mg/kg b.w., subcutaneous injection) to induce the small intestinal injury. After the injection of indomethacin for 12 h, the mice were given by gavage with 1 g/kg b.w. of deionized water (the Indo group), nZnO (the Indo-nZnO groups) and mZnO (the Indo-mZnO groups). The normal mice were also administered with deionized water (the control group), nZnO (the nZnO group) and mZnO (the mZnO group) at a single dose of 1 g/kg b.w. by gavage. The mice were sacrificed at 4 h, 12 h and 24 h post gavage and the blood samples were collected. The heart, liver, spleen, stomach, kidneys, lungs, brain, and small intestine were dissected and collected. Segments of tissues from liver, kidneys and small intestine of each group were preserved in 4% formalin for histopathological examination.

2.7. Zn, Fe and Cu contents in tissues of mice

Certain amounts (0.1–0.5 g) of tissues (blood, liver, kidneys, spleen, lungs, brain and small intestine) were digested with HNO₃ and H₂O₂ by the microwave digestion system. Then, the digested solution was heated at 180 °C to remove the residual HNO₃ until it was colorless and clear. The remaining solution was adjusted to 5 ml with 2% HNO₃ solution and the contents of Zn, Fe and Cu were determined by the ICP-MS. The final contents reported were normalized based on the tissue weight. The same process without tissues was performed to prepare the blank samples.

2.8. Serum biochemical parameter assay

The whole blood samples were centrifuged at 3000 rpm for 15 min to collect serum. The serums were frozen at -20 °C until use. The biochemical assays were performed on a Clinical Automatic Chemistry Analyzer (Hitachi 7080, Japan). Alanine aminotransferase (ALT), aspartate aminotransferase (AST), lactate dehydrogenase (LDH), blood urea nitrogen (BUN), creatinine (CREA), uric acid (UA) and total bilirubin (TBIL) were measured by using the commercial kits (The Seno Clinical Diagnostic Products Co., Japan).

2.9. Histopathological examination

For pathological examinations of liver, kidney and intestine, tissues were embedded in paraffin blocks, then sliced into 5 µm in thickness and placed onto glass slides. After hematoxylin-eosin (HE) staining, these slides were investigated under an optical microscope (DMI750, Leica, Germany) and photos were captured by the camera.

2.10. µ-XRF studies of intestine samples at SSRF

µ-XRF mappings of the distribution of Zn in the mouse intestine were performed with an incident energy of 9.700 keV at beamline LU15 at the Shanghai Synchrotron Radiation Facility (SSRF, Shanghai, China). The small intestine samples collected from mice of all groups were frozen at -80 °C for several minutes and then embedded in OCT (optimal cutting temperature compound, Richard-Allan Scientific Neg-50, Thermo, USA). Later, they were axially sectioned (7 µm in thickness) with a Cryostates (Microm HM525, Germany) at -20 °C and mounted onto a Mylar film for analysis. The fluorescence signal was detected by a Si drift detector. Two photodiodes were used to measure

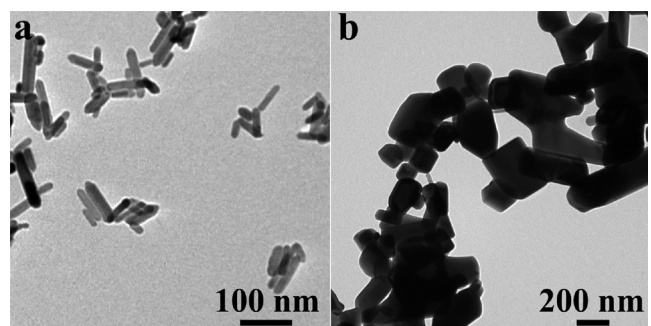


Fig. 1. Representative TEM images of nZnO (a) and mZnO (b).

the incident and transmitted beam intensities. Fluorescence signals were collected for each point with a step of 5 µm × 5 µm. The data were processed using Igor Pro software. The fluorescence intensities were normalized to the incident X-ray intensity to estimate the relative Zn content.

2.11. Statistical analysis

All data were calculated from at least three independent experiments, and are presented as the mean ± standard deviation (mean ± SD). Analysis of statistical significance was done using the Student's t-test. The difference was considered significant if P < 0.05.

3. Results

3.1. Physicochemical properties of ZnO NPs

The commercial nZnO and mZnO were characterized before animal experiments. nZnO NPs were in rod shape, with a size of around 20 nm × 100 nm (Fig. 1a), while mZnO NPs were cubic shape particles, with a size of ~200 nm (Fig. 1b). Nanomaterial is usually defined as a material with at least one dimension size range from approximately 1–100 nm, while size upper boundaries vary in different fields (Boholm and Arvidsson, 2016). Therefore, both nZnO and mZnO were defined as nanoparticles in this study. Both samples were in the wurtzite phase crystal according to the XRD patterns. XRF analysis indicated that the purities of nZnO and mZnO were 98.5% and 99.9%, respectively, and the main impurities were Si and Al.

ZnO NPs tended to aggregate in water. DLS measurements showed that the hydrodynamic diameter of nZnO (1636 ± 133 nm) was slightly larger than that of mZnO (1107 ± 278 nm). The zeta potentials of nZnO and mZnO were -8.6 ± 1.7 mV and -16.7 ± 3.7 mV, respectively, which were consistent with the results of hydrodynamic diameters of these NPs. A severer aggregation of ZnO NPs was observed in the simulated gastric juice and the aggregation alleviated after they were dispersed in the intestinal juice, which is accordance with the previous study (Gerloff et al., 2013). However, DLS could not provide precise results in the differences of size distributions of these two ZnO NPs in gastric and intestinal juices, because of the very similar size distributions of simulated juices alone and ZnO NPs in simulated juices. In addition, we note that DLS is not a perfect technique to measure the size of the non-spherical shape particles due to the measurement mechanism of DLS. Therefore, we mentioned the TEM size of particles in this study. According to TEM images (Fig. 1), from three dimensions, nZnO is smaller than mZnO.

The dissolved fractions of ZnO NPs in the simulated digestion juices are summarized in Table 1. ZnO NPs barely dissolved in water. In the gastric juice, over 10% of ZnO dissolved. The lower solubility of nZnO corresponded with the severer aggregation of nZnO. However, the dissolved fraction in the intestinal juice decreased dramatically to less than 2%, and there was no significant difference between the two ZnO

Table 1
Dissolution of ZnO samples in water and the simulated digestion juice.

Sample	Test system	Dissolved fraction (%)
nZnO	water	0.035
	simulated gastric juice	10.6
	simulated gastric and intestinal juice	1.72
mZnO	water	0.040
	simulated gastric juice	14.2
	simulated gastric and intestinal juice	1.89

NPs. This indicated that part of dissolved Zn in stomach precipitated after entering the intestine.

3.2. Developing the IBD mice by indomethacin

Subcutaneous injection of indomethacin induced the damage to the intestine, which is a well-accepted method to develop the IBD mice model (Bradley et al., 1982; Kawahara et al., 2011; Randhawa et al., 2014). As shown in Fig. S1, the MPO activity of small intestine, an index of neutrophil accumulation to characterize the intestinal inflammation and injury, was significantly increased after subcutaneous injection of indomethacin (9 mg/kg b.w.). Furthermore, we adopted TEM to visibly investigate the small intestinal samples directly. Compared to the normal intestine, the shortening and disorder of the villi, loss of cell membrane, and evident cell apoptosis and necrosis were observed in the intestine of IBD mice (Figs. 2 and S2), confirming the intestinal injury. The increased MPO activity and significantly changed intestine morphology indicated that the IBD mice model was successfully developed by the indomethacin treatment.

3.3. Distribution of Zn in mice after gavage exposure to ZnO samples

To measure the Zn content, the blood and main organs were collected at different time points after oral administration of a single dose of ZnO NPs (1 g/kg b.w.) to normal mice and IBD mice, and the results are shown in Figs. 3 and 4. As shown in Fig. 3, the concentrations of Zn in the blood, liver, kidneys, spleen, and lungs were significantly increased at 4 h and 12 h after nZnO administration (Fig. 3a and b), while no uptakes of Zn in the brain in the normal mice. At 24 h, the accumulation of Zn could only be detected in liver and kidneys, while the Zn level in blood, spleen and lungs restored to the background level (Fig. 3c). This results clearly showed the uptake of Zn after oral administration of ZnO NPs, and fast recovery of Zn levels in mice within 24 h. mZnO showed similar uptake contents as nZnO in all organs (Fig. 3d). By contrast, the concentrations of Zn in the blood, liver, kidneys, spleen and lungs increased greatly during 24 h after nZnO administration in the IBD mice (Fig. 3). Distinguished to the normal

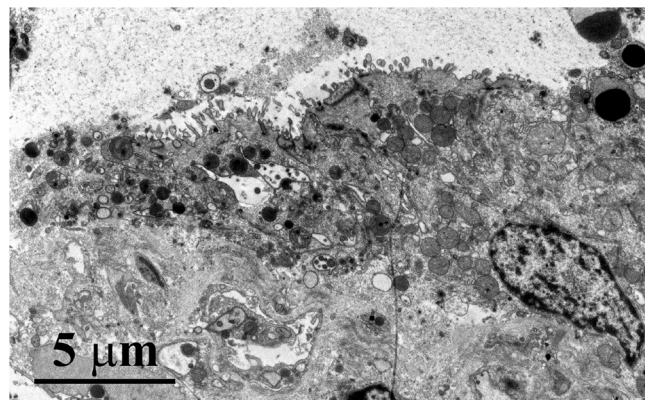


Fig. 2. TEM investigation of the indomethacin-induced changes in the small intestine of mice.

mice, the increased Zn levels in all organs could still be observed at 24 h postexposure, indicating a slower recovery of Zn levels in mice. In addition, the distribution pattern of administrated mZnO was similar to nZnO in the IBD mice, except for much higher hepatic Zn level and lower Zn levels in other organs.

Comparing the distributions of Zn in normal and IBD mice after ZnO administration, the most significant difference was the Zn content in the liver. IBD mice induced much higher hepatic Zn level than normal mice. In other tissues, the difference was not significant. It also should be noted that bigger particles showed higher hepatic Zn accumulation and slightly lower Zn accumulation in other tissues.

To sum up, these results imply the intestinal injury/inflammation could significantly affect the hepatic Zn distribution in mice. In addition, the size effect was observed in this study, though the Zn distribution profiles in organs postexposure to nZnO and mZnO were very similar. The intestinal injury/inflammation allowed more Zn enter the liver of mice, especially for larger ZnO particles.

It is well known that the absorption of various substances in gastrointestinal tract mainly occurs in the small intestine. Therefore, the Zn levels in the small intestine at 12 h postexposure to ZnO samples were also measured. As shown in Fig. 4, both the normal and injured mice showed absorption of Zn by the small intestine after ZnO exposure. In the normal mice, small intestinal Zn contents in the nZnO and mZnO groups were almost same. But the Zn content was higher in the IBD mice when exposed to nZnO than mZnO. To eliminate the interference from attached ZnO particles, all substances in intestines were removed and the cut-opened intestines were rinsed by phosphate buffer solution before measuring Zn. This may be ascribed to the fact that little small particles might enter the intestine through the injured spots, resulting in higher Zn content in the injured intestine postexposure to nZnO. This was confirmed by the μ -XRF mapping of Zn of the intestine (Figs. 5 and S3). From the μ -XRF image of the injured intestine (the Indo-ZnO group), Zn displayed the punctate distribution (Fig. 5c and d), especially in the Indo-nZnO group (Fig. 5d). Compared with the ZnO treated mice, the Zn level in the intestine of both normal mice and IBD mice was lower (Fig. S3), which was consistent with results in Fig. 4. Combined with the result of much different Zn contents in livers, it is reasonable to assume that the ZnO particles could cross intestine and enter the circulatory system. Certainly, it is also possible that the smaller particles were absorbed strongly onto the intestine and very difficult to be washed away, then resulted in higher Zn content in the intestine of the Indo-ZnO group.

3.4. Effect of gavage exposure to ZnO NPs on the distribution of iron and copper in mice

The absorption of certain metal element may affect the absorption and distribution of other metal elements in animals. To evaluate the influence of ZnO particles exposure, the distribution of essential element Fe and Cu in tissues in both normal and IBD mice were measured by ICP-MS (Figs. 6–8).

Compared to the normal mice, the IBD mice presented a decreased concentration of Fe in the blood, in kidneys at 12 and 24 h, and spleen at 24 h. No significant effect was observed in other organs (Fig. 6). The concentrations of Fe in mice after treatment with nZnO and mZnO were similar at 12 h postexposure. In the normal mice, after nZnO administration, an enriched Fe level in the blood and slight increase in liver were observed at all time points after nZnO administration (Fig. 6). In addition, slight decreased Fe levels in the kidneys, spleen and lungs were observed within 24 h (Fig. 6). The variations of Fe distribution along with the time were very small. However, a significant difference was found between the nZnO and mZnO exposure groups. In addition, the Fe levels in the liver, kidneys, spleen, lungs and brain in the mZnO group increased markedly, compared to the nZnO group at 12 h postexposure.

In the IBD mice, the level of Fe in the blood increased numerously at

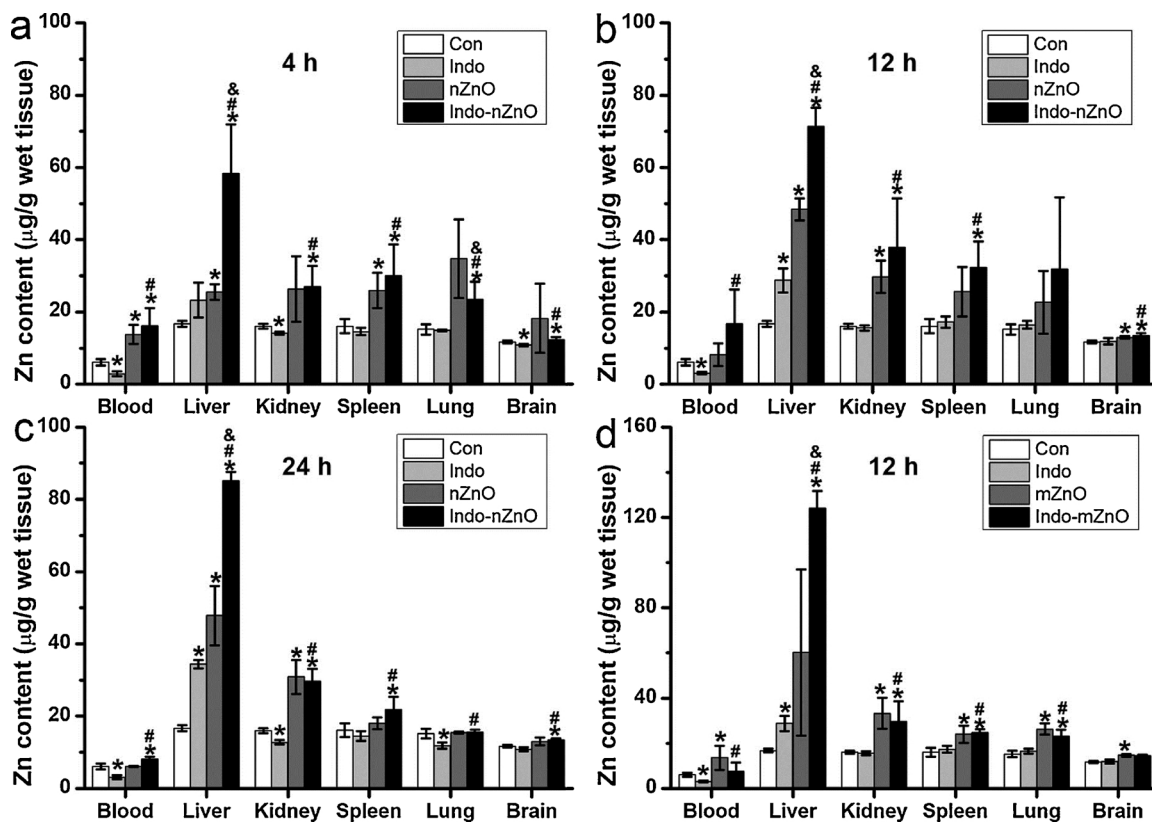


Fig. 3. The Zn contents in organs of mice at 4 h, 12 h and 24 h after oral exposure to ZnO particles ($n = 3-4$). (a, b and c) mice were exposed to nZnO; (d) mice were exposed to mZnO. *, #, & Significant difference at $P < 0.05$, in which * compared with the normal control, # compared with the Indo group, and & compared with the ZnO group.

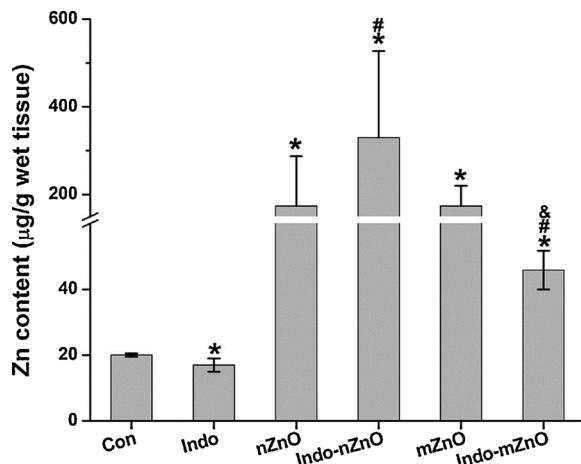


Fig. 4. The Zn content in the small intestine of mice at 12 h post exposure to ZnO NPs ($n = 3-4$). *, #, & Significant difference at $P < 0.05$, in which * compared with the normal control, # compared with the Indo group, and & compared with the ZnO group.

4 h after the nZnO administration, then dropped to normal level at 24 h postexposure (Fig. 6). The Fe in the liver increased before 12 h and went back to normal level at 24 h; while that level in the spleen dropped first at 4 h and then restored to normal after 12 h postexposure. No changes were observed in other organs, compared to the indo control. The differences between the nZnO and mZnO exposures were very similar to that in the normal mice. Compared to nZnO, mZnO induced the increased accumulation of Fe in several organs.

The distributions of Fe in normal and IBD mice after ZnO administration were very comparable. Along with time, the Fe level was

slightly higher in the IBD mice. No other difference was found between nZnO and mZnO exposures in normal mice and IBD mice.

As for the Fe content in the intestines, it decreased significantly in normal mice after being exposed to both ZnO particles, while slight, but not significant, increases were observed in the IBD mice (Fig. 7), i.e., Fe levels in intestines were higher in IBD mice than in normal mice after ZnO exposures. The intestinal injury/inflammation augmented the absorption of Fe from intestines.

Clearly, the Fe distributions in both the normal and IBD mice could be affected by ZnO exposure. The trend of Fe distributions between the Indo-nZnO group and nZnO group was similar. Regardless of whether mice had an intestinal injury/inflammation, the size effect of ZnO on the Fe distribution was obvious. Compared to nZnO, mZnO significantly increased Fe in various organs, except for in blood.

Figs. 7 and 8 showed the distribution of Cu in mice. Compared with the normal control, the increased levels of Cu in blood and livers at 12 h and 24 h postexposure and the decreased level Cu in kidneys were observed in IBD mice. No other significant Cu changes were found. In the normal mice, at 4 h after nZnO administration, the level of Cu in liver and spleen increased (Fig. 8a). Along with the time, Cu level in other organs also increased except in blood and kidneys (Fig. 8b and c). For the IBD mice, Cu level in all organs except for blood increased greatly at all three time points after nZnO administration (Fig. 8). In blood, Cu decreased at 12 h and 24 h postexposure. mZnO induced similar Cu distribution changes in both normal and IBD mice as nZnO, with higher accumulation in kidneys and lower accumulation in the spleen.

Both the ZnO exposure and the intestinal injury/inflammation led to the decrease of Cu level in the small intestine (Fig. 7). However, the intestinal injury/inflammation decreased Cu level only in the small intestine postexposure to nZnO, as no such significant decrease was observed in postexposure to mZnO. This indicates that the higher level

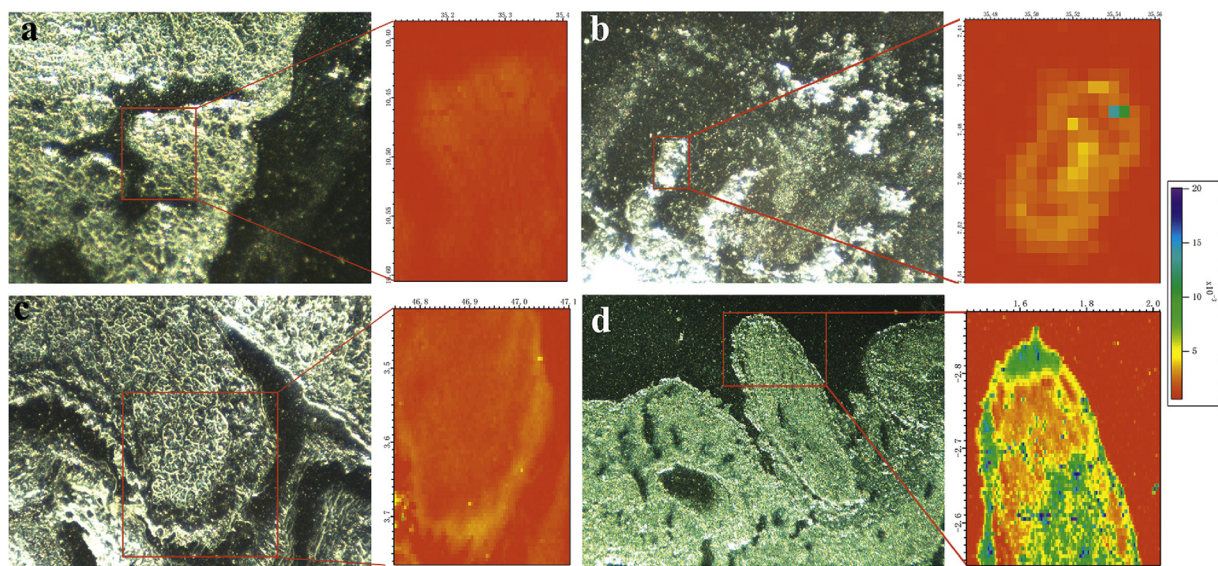


Fig. 5. Images of the transversal section of mouse intestine at 12 h postexposure to mZnO (a and c) and nZnO (b and d). (a) the mZnO group; (b) the nZnO group; (c) the Indo-mZnO group; (d) the Indo-nZnO group. In each panel, the left picture is the photo image of the small intestine; the right picture is the corresponding μ -XRF map, showing the normalized Zn intensity of part of the square in the left picture. The Zn intensity scale is shown in the right side of images, in which dark blue represents higher Zn intensity and red represents the absence of a Zn signal. (For interpretation of the references to colour in this figure legend, the reader is referred to the web version of this article).

of Zn in the small intestine interfered with the absorption of Cu after nZnO exposure.

Comparing Cu data between the Indo-nZnO group and nZnO group, the intestinal injury induced transient increases of Cu level in liver, spleen, lungs and brain at 4 h postexposure. After 4 h, no significant Cu

changes were observed.

3.5. Biochemical assay of serum

The changes of serum biochemical parameters of mice postexposure

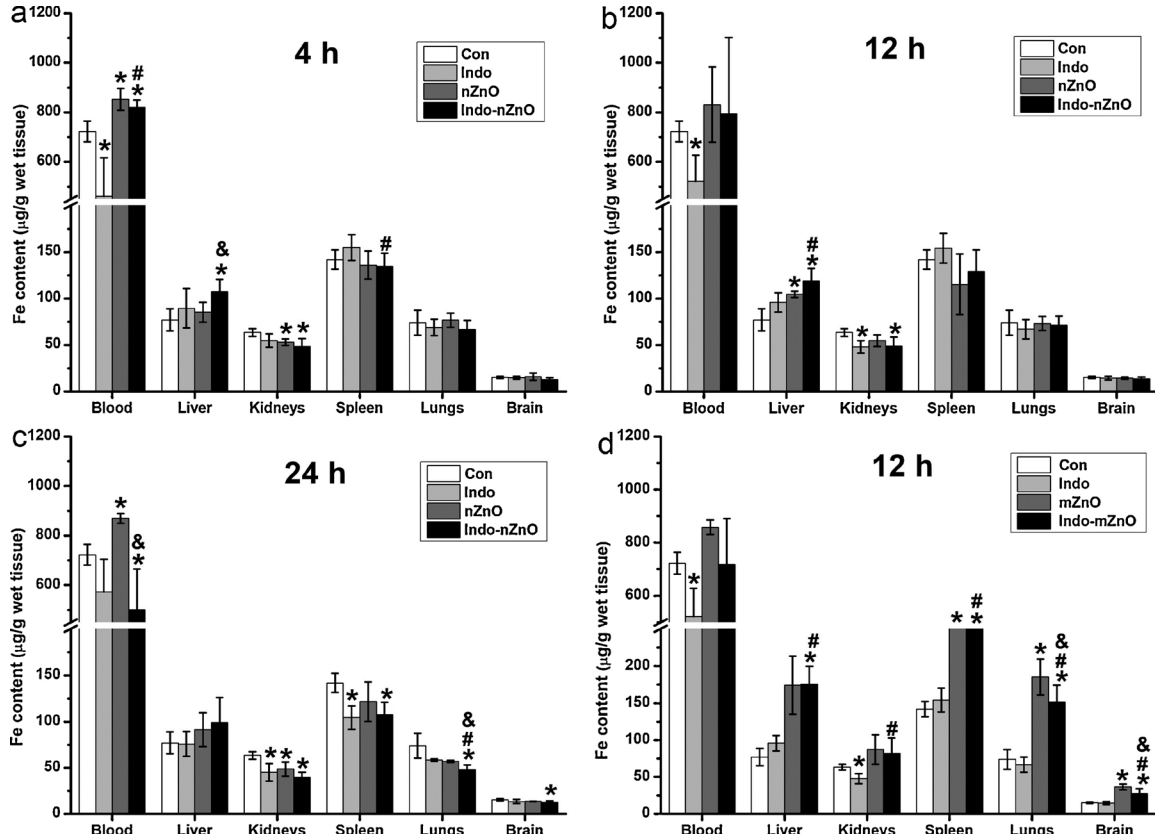


Fig. 6. The Fe distribution in mice at 4, 12, 24 h postexposure to ZnO samples (n = 3–4). (a–c) mice were exposed to nZnO; (d) mice were exposed to mZnO. *, #, & Significant difference at P < 0.05, in which * compared with the normal control, # compared with the Indo group, and & compared with the ZnO group.

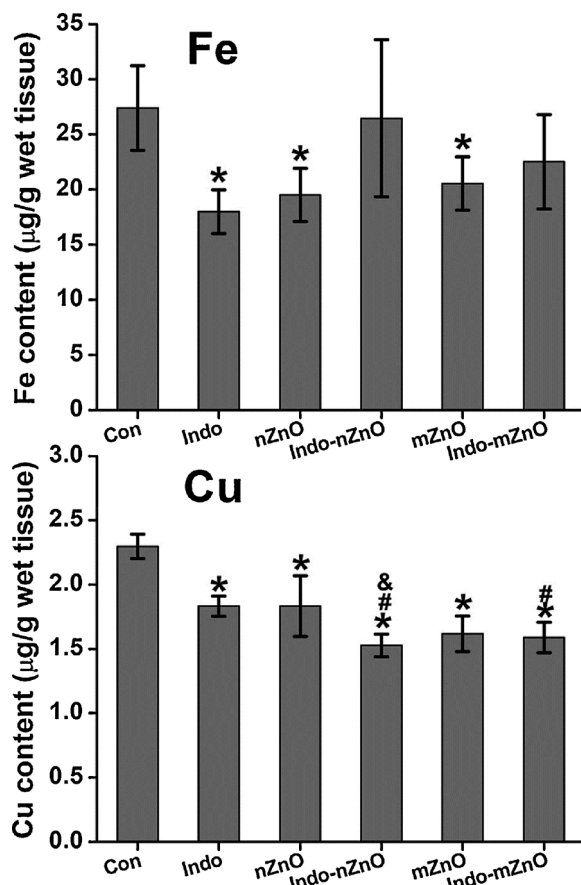


Fig. 7. The contents of Fe and Cu in the small intestines of mice at 12 h post gavage exposure ($n = 3-4$). *, #, & Significant difference at $P < 0.05$, in which * compared with the normal control, # compared with the Indo group, and & compared with the ZnO group.

to ZnO NPs have been summarized in Fig. 9. In the IBD mice, the levels of liver biomarkers ALT, AST and ALP decreased at all three time points, while LDH and TBil levels decreased only at 24 h. As for kidney biomarkers Crea, UA and BUN, there was little change, except for a slight decrease of Crea at 12 h and of BUN at 24 h.

In the normal mice, after the nZnO administration, ALT and AST levels increased first and returned to the baseline at 24 h; ALP, LDH and TBil levels did not change at all time points. Most Crea, UA and BUN levels remained unchanged, except that of UA and BUN at 4 h. The mZnO group showed the same patterns as the nZnO group, except a higher UA value was found in the mZnO group.

In the IBD mice, most parameter (ALT, AST, ALP and LDH) levels increased if compared with the Indo control after the nZnO administration. As for Crea, UA and BUN, they increased at 4 h, and decreased later on. At 24 h, lower UA level was observed. Different from nZnO, mZnO induced increases of ALT and AST, and decreases of LDH and TBil at 12 h.

Comparing these parameters between the nZnO group and Indo-nZnO group, we found that the intestinal injury lowered ALP and TBil, and increased Crea at the beginning, then lowered ALT, ALP, TBil and UA at 24 h. Parameters changed more significantly for the Indo-mZnO group.

These results indicated that the intestinal injury/inflammation had a greater impact on the biological parameters in mice than ZnO exposure. In addition, the particle size slightly affected on these biological parameters.

3.6. Histopathological investigation

The histopathological investigation indicated very limited organ damages in the livers and kidneys. Some cell fusions were found at the edge of livers in the Indo group at 12 h. In the Indo-nZnO group, some cell degeneration/necrosis in livers (Fig. S4) and tubule hyperplasia (Fig. S5) in kidneys were observed.

Compared with the normal intestine, the IBD mice presented intestinal mucosa abscission, glands erosion, glandular atrophy, lymphocyte with inflammatory infiltration, levels disturbance, fibrous tissue hyperplasia and inflammation, which were more serious than that induced by ZnO NPs and covered up the impacts of ZnO NPs on intestines (Fig. 10). There was no obvious difference between lesions induced by nZnO and mZnO.

4. Discussion

In this study, alteration of bioeffects of orally administrated ZnO NPs in the IBD mice has been carefully examined. Significantly high hepatic accumulation of Zn in the IBD mice was observed after ZnO NPs exposures. In addition, the distributions of Fe and Cu in the IBD mice shifted. Nevertheless, the toxicity of ZnO NPs did not change in the IBD mice, for the intestinal injury/inflammation induced more serious damages to mice. Compared the bioeffects of nZnO and mZnO, distinct size effect was observed. Two ZnO NPs showed similar distribution trends, but notable different content values, in which mZnO possessed higher accumulation ability than nZnO in some organs (Fig. 3).

With increasing number of nano-enabled products, the oral exposure of NPs to human beings is inevitable. ZnO NP is one of the most popular NPs and their bioeffects after oral administration have been widely studied. The toxicity and distribution of ZnO NPs in vivo were reported from different viewpoints. However, most of these studies focused on the normal animals without considering their health status. The gastrointestinal tract is the first step and the location of nutrient absorption for NPs entering a body after the oral administration. If the gastrointestinal tract was damaged, it may affect the absorption and toxicity of certain agents. It hence becomes interesting to investigate whether and how the intestinal injury/inflammation could influence the distribution and toxicity of ZnO NPs. Considering the fact that the size of NPs is a determinant for their biological behaviors, we used two ZnO NPs, smaller nZnO and bigger mZnO.

Because no guideline for the risk assessment of ZnO NPs has been approved, we chose the ZnO dose consulting the reference dose of zinc (8–18.6 mg/kg b.w./day for zinc) reported by US Food and Drug Administration (FDA, 2002). Thus, the corresponding mouse dose is 98–229 mg/kg b.w./day for Zn, or 123–285 mg/kg b.w./day for ZnO equivalently after considering the conversion coefficient of 12.3 from the human dose to the mouse dose (FDA, 2005). Note that we only performed a single gavage, therefore 1 g/kg b.w. was adopted as the administration dose.

Similar to published reports that orally-administrated ZnO induced the increase of Zn level in blood and other organs, especially in the target organ liver (Li et al., 2012; Sharma et al., 2012; Umrani and Paknikar, 2014 Wang et al., 2008). The increased level of Zn in blood and other organs in both normal and IBD mice has been observed in this study (Fig. 3). The intestinal injury/inflammation clearly increased the Zn level in liver; while in other organs, the level of Zn increased slightly at 12 h postexposure, and then returned to the background level at 24 h. The possible reason is that intestinal injury made the intestine permeable to nanoparticles, and the liver is the target organ of ZnO particles. In addition, a much higher increment of Zn in liver was observed in the Indo-mZnO group than in the Indo-nZnO group (Fig. 3b and d). It was also found that the recovery of Zn level back to the background in organs needed more time in IBD mice, further supporting that intestinal injury did influence the uptake of ZnO NPs.

The distribution data of Zn in mouse organs indicated that only a

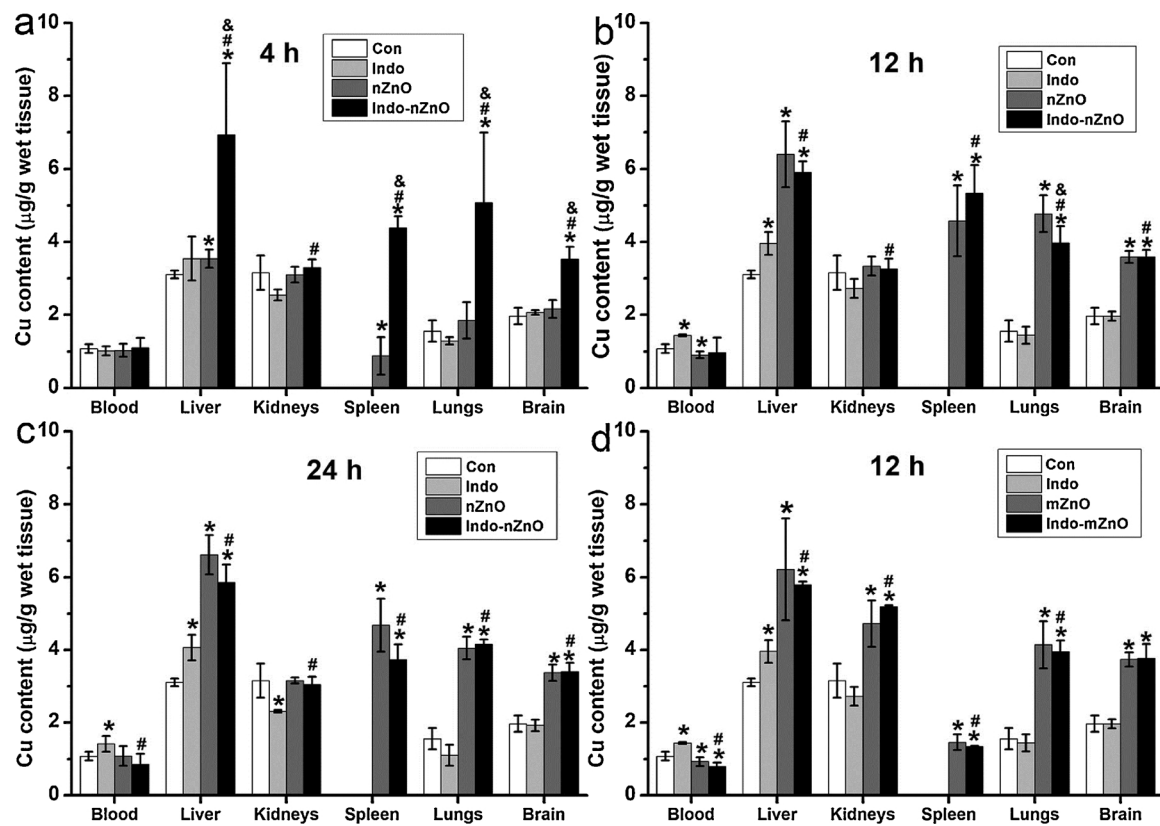


Fig. 8. The Cu distribution in mice at 4, 12, 24 h post exposure to ZnO samples ($n = 3-4$). (a-c) mice were exposed to nZnO; (d) mice were exposed to mZnO. *, #, & Significant difference at $P < 0.05$, in which * compared with the normal control, # compared with the Indo group, and & compared with the ZnO group.

small amount of ZnO NPs passed through intestines, even when the mice suffering with IBD. This result was also consistent with the previous report by Lee et al. (2012). They found that only less than 5% particles crossed the intestinal barrier after a single dose of 250 mg ZnO NPs /kg b.w. (Lee et al., 2012). Li et al. confirmed that 6.48–32.49% of administrated ZnO entered into blood; smaller particles showed higher uptake (Li et al., 2012). However, we demonstrated that the injury improved the possibility of the particles passing through intestines. As shown in the μ -XRF image (Fig. 5), many small spots with much higher Zn concentrations were observed, indicating the existence of nZnO in the injured intestines (Fig. 5d). Such phenomenon was not found in normal mice (Fig. 5b). Compared with mZnO (Fig. 5c), more nZnO particles were observed in intestines, possibly because smaller particles might enter the intestine through the injured spots and the attached bigger mZnO particles were easier to be moved away when we cleaned the inside of intestines. Separately, one mZnO particle was around one hundred times heavier than one nZnO particle, i.e., one mZnO particle may result in similar zinc accumulation in liver as a hundred of nZnO particles. This may explain that higher accumulation of Zn in liver was observed in mZnO group than in the nZnO group in IBD mice. This differed from the results of most published papers, that smaller particles make higher uptake in organs (Baek et al., 2012; Li et al., 2012). The finding confirms that special biological situation of animals would affect the bio-consequence of the administrated foreign agents.

Trace element Fe and Cu are essential to maintain human health (Mertz, 1981). They are indispensable for a lot of proteins and enzymes, which are necessary for normal physiological functions, and therefore their deficiency results in serious diseases in human subjects. In the meantime, the excess of Fe and Cu also means health problems. For example, the overdose of Fe is closely related to cancer, liver diseases etc. Keeping essential trace element balance is very important for the health. After exposure to ZnO NPs, not only the Zn contents in organs changed, but the contents of two essential metal elements, Fe and Cu,

also changed (Figs. 6–8). In the IBD model, the change trends of Fe and Cu distributions were similar to those of the corresponding ZnO group in normal mice after ZnO NPs exposures. It is highly possible that such trace elements changes owe to the different distributions of Zn in mice.

Besides the intestinal injury may alter the distributions of the Fe and Cu, absorption of ZnO NPs may interact with absorption of Fe and Cu by altering other absorption mechanisms (e.g. metal transporters) (Scheers, 2013). For instance, in Caco-2 cells, Zn could increase the uptake and transepithelial flux of Fe via regulating the iron transporters (DMT1, IREG1) (Yamaji et al., 2001; Scheers, 2013). Although many researchers found that Zn inhibited the absorption of Fe and Cu, conflicting data and varied mechanisms on interactions among Zn, Fe and Cu have also been reported, indicating the complexity of interactions (Storey and Greger, 1987). There are many factors influencing the results, such as the relative amount and form of these elements in diets, diet composition, species, design of study (test time points, acute or chronic exposure) (Scheers, 2013). For example, non-heme Fe depressed the absorption of Zn when Zn was administrated in an inorganic form, but did not depress when Zn was in an organic form (Scheers, 2013). Therefore, exposure to ZnO NPs and other Zn containing species may have different effects on the mineral levels *in vivo*. Wang et al. reported that orally administrated ZnO NPs did not affect the Fe and Cu levels in mice (Wang et al., 2016, 2017). The possible reason for the conflicting results with ours is the much different exposure periods, which affect the elaborate regulation of Fe and Cu *in vivo*. It could be expected, the changed Fe and Cu distribution may recover along with time if such changes did not induce irreversible damages.

Without exception, liver is the most common deposition location for ZnO NPs in this study. The higher accumulation of Zn in liver was observed in mZnO group than in the nZnO group, especially in IBD mice (Fig. 3). The second most accumulation organ is kidney (Fig. 3). Wang et al. reported a significant increase of Zn contents in kidneys and slight increase in liver after a single dose of 5 g/kg of ZnO NPs (Wang et al.,

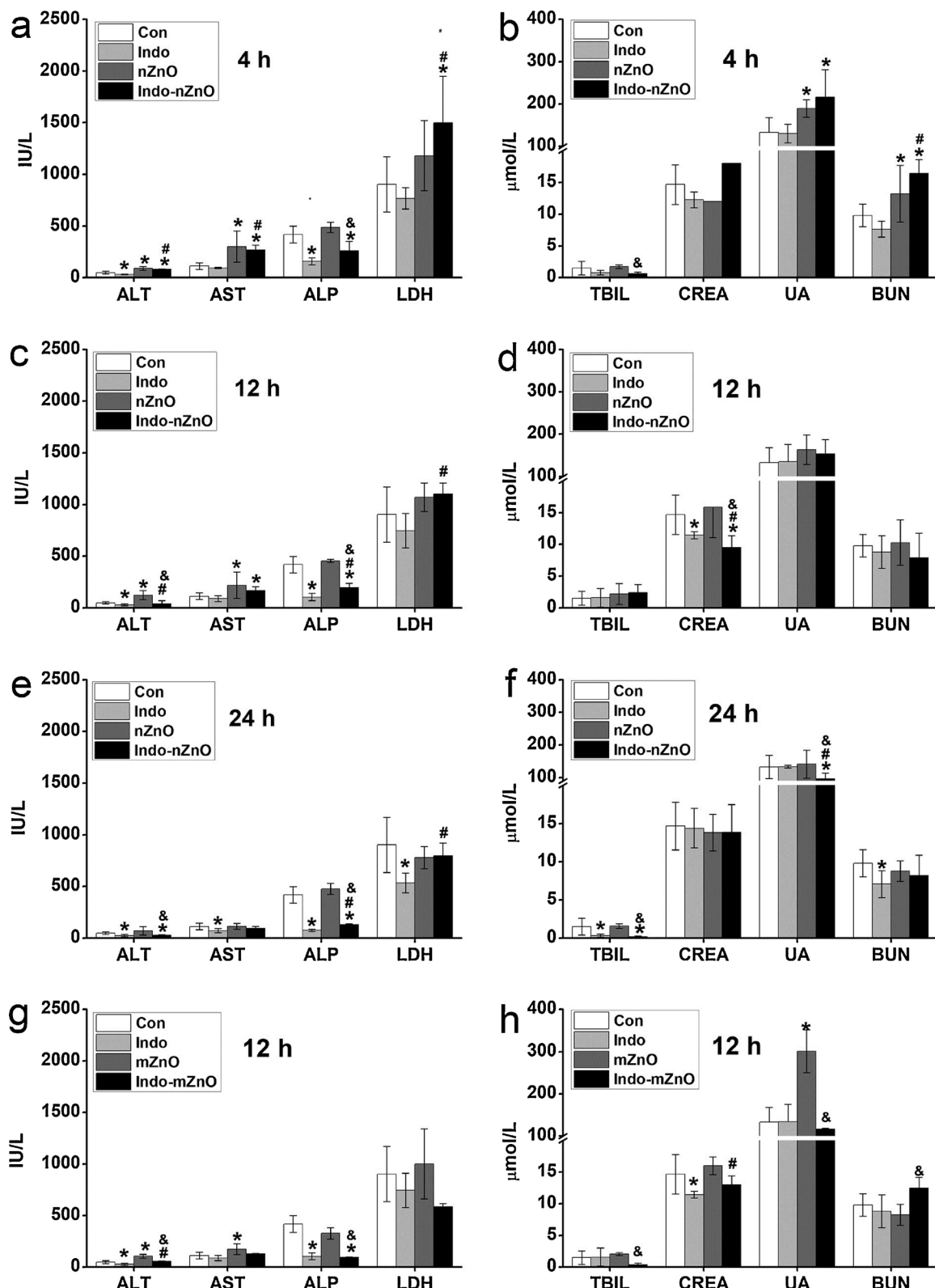


Fig. 9. The influence of ZnO samples on the serum biochemical parameters of mice ($n = 3-4$). (a–b) nZnO, 4 h postexposure; (d–c) nZnO, 12 h postexposure; (e–f) nZnO, 24 h postexposure. *, #, & Significant difference at $P < 0.05$, in which * compared with the normal control, # compared with the Indo group, and & compared with the ZnO group.

2008). Li et al. found that Zn mainly distributed in liver, spleen and kidneys (Li et al., 2012). However, no difference was found in the accumulation of Zn in kidneys between the mZnO group and nZnO group (Fig. 3b and d). This also indirectly proved that the liver is the first

target of ZnO NPs.

It was reported that liver damage was the predominating damage induced by ZnO NPs, which was revealed by the histopathological examination and enzyme levels change in serum (Esmaeilou et al., 2013;

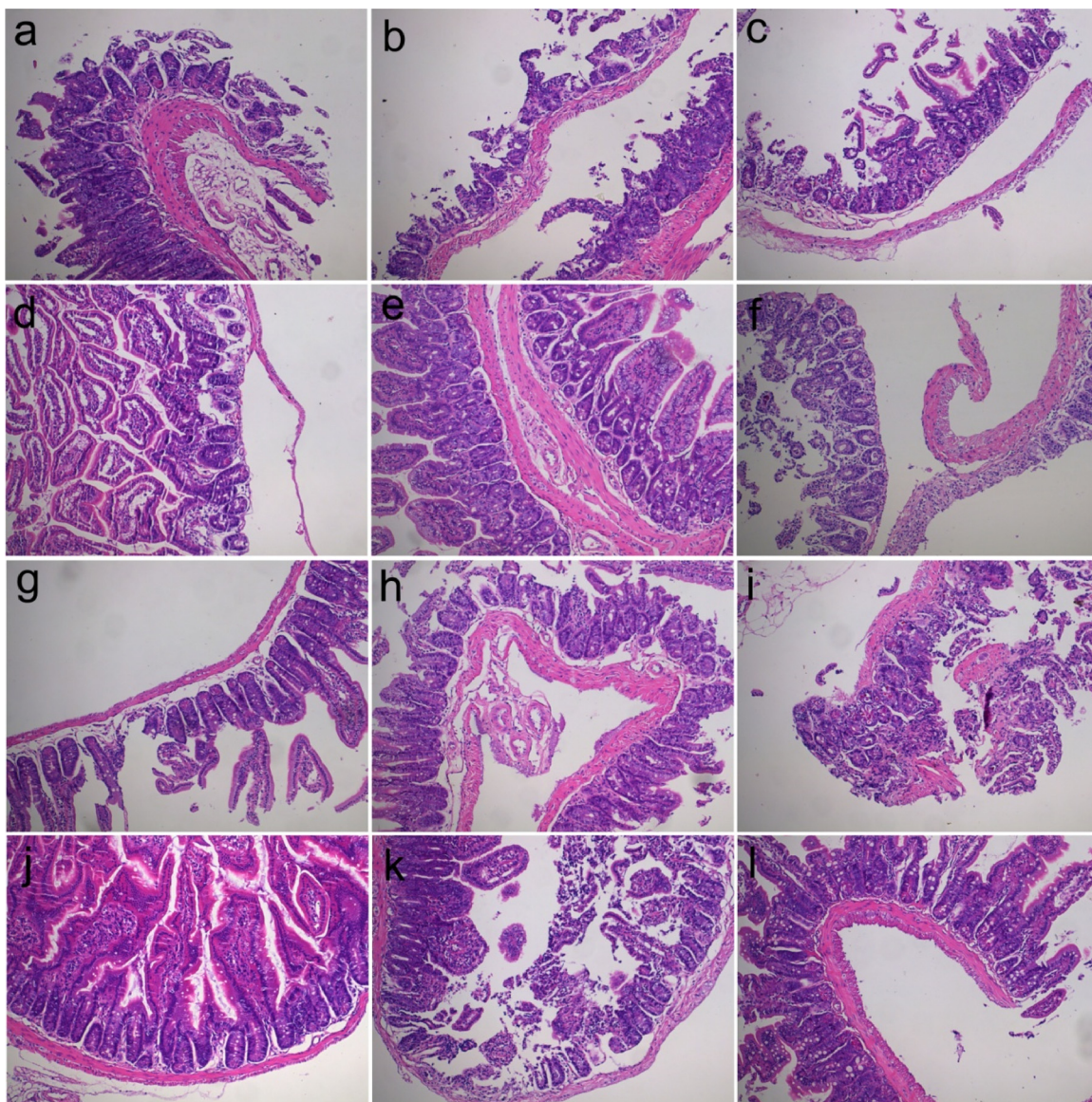


Fig. 10. Histopathology of the small intestine (100×) of mice at different time points postexposure to ZnO samples. (a) the Indo group at 4 h, (b) the nZnO group at 4 h, (c) the Indo-nZnO group at 4 h, (d) the Indo group at 12 h, (e) the nZnO group at 12 h, (f) the Indo-nZnO group at 12 h, (g) the Indo group at 24 h, (h) the nZnO group at 24 h, (i) the Indo-nZnO group at 24 h, (j) the control group, (k) the mZnO group at 12 h, (l) the Indo-mZnO group at 12 h.

Li et al., 2012; Sharma et al., 2012; Srivastav et al., 2016; Wang et al., 2008). Li et al. observed slight transient liver histopathological lesions after a single dose exposure of 2.5 g/kg of ZnO NPs (Li et al., 2012). Similarly, Sharma et al. reported liver damage in mice revealed by the histopathological examination and increased enzyme levels in serum (ALT and ALP) (Sharma et al., 2012). Esmaeilou et al. (2013) reported serious liver damage in rats corroborated by the changed biological indices in serum, hepatocyte necrosis and pathological observations. In this study, slight liver damage was found by the pathological observation and some biological parameter changes were observed in IBD mice, indicating the slight toxicity of ZnO NPs to liver of IBD mice (Figs. 9 and S4). Besides, the kidney was reported as a target organ for ZnO NPs (Esmaeilou et al., 2013; Hong et al., 2013). Although no obvious damage in kidneys was detected by pathological observations (Fig. S5), the changes of the biological parameters were observed (Fig. 9), indicating a little toxicity of ZnO NPs to kidneys. Lesions in intestines were observed, which was mainly due to the injury induced by indomethacin.

It has been reported that, besides size and dosage, the dissolution

property of ZnO particles is also a key factor in determining their fate in biosystems (Yang et al., 2010). Some studies contended that the dissolved Zn from ZnO NPs was preferentially absorbed into systemic circulation. Baek et al. (2012) concluded that orally administrated ZnO NPs were absorbed in an ionic form rather than in the form of particulates. Cho et al. (2013) attributed the higher absorption of 40 nm ZnO NPs in rats to the higher dissolution rate of NPs to ions in acidic gastric juice. Umrani et al. and Hong et al. also stated that Zn ions dissolved from ZnO NPs would induce the distribution and toxicity (Hong et al., 2013; Umrani and Paknikar, 2014). In this study, we measured the solubility of ZnO samples in simulated digestion juice. It was found that over 10% ZnO NPs dissolved in the stomach juice, however, the dissolved fraction of ZnO NPs dropped to around less than 2% after ZnO NPs entering intestine juice. This indicated that the soluble Zn tract was not the only source of the Zn uptake by mice. It is possible that those small particles/aggregations of Zn also made a contribution, referring to the small spots expressing the concentrated Zn in the μ -XRF image of the intestine (Fig. 5d). This is supported by Kim et al., who found that bulk ZnO particles were more bioavailable in the body than ZnO

nanoparticles, though the particle size did not affect dissolution properties of ZnO particles (Kim et al., 2016).

Besides size, the shape of NPs may also be a factor influencing the distribution profile of two ZnO NPs. nZnO was the long rod shape and mZnO was the cubic shape. The different shapes suggest different contact surface areas and possible interaction direction between ZnO and biospecies, such as cells, in mice. It has been reported that ZnO nanorod appeared to be more damaging compared with spherical one on bacteria, due to the increased probability of mechanical damage caused by nanorods and cell walls (Matula et al., 2016). Similarly, higher cellular uptake of rod-shaped nanoparticles than spherical and cubic ones was reported (Banerjee et al., 2016; Niikura et al., 2013). Considering the dissolutions of two ZnO NPs were very similar in simulated gastric and intestinal juices, we thought there was no difference in contact surface area between two ZnO NPs. The different distribution of ZnO NPs in intestine indicated that the rod nZnO was easier to contact with intestine than cubic mZnO.

5. Conclusions

Herein, the effect of the intestinal injury/inflammation on the distribution and toxicity of orally administrated ZnO NPs in mice has been investigated. The results indicate that the mice with IBD present distinguish uptake of ZnO NPs and the levels of essential trace element Fe and Cu. In the IBD group, much higher Zn content in the liver was detected. Bigger ZnO NPs resulted in the higher accumulation in organs than smaller ones. The combined results of pathological investigation and biological parameters demonstrated that ZnO NPs induced a little organ damages in IBD mice. The gastrointestinal tract related diseases are widely distributed in populations. The findings of this work indicate that these diseases change the distribution and toxicity of the exotic engineered nanomaterials, which may enhance the potential concerning of toxicity of these nanomaterials.

Conflict of interest

The authors report no conflicts of interest. The authors alone are responsible for the content and writing of the paper.

Transparency document

The Transparency document associated with this article can be found in the online version.

Acknowledgements

We thank the National Natural Science Foundation of China (Nos. 31771105 and 31571024) and the National Basic Research Program of China (No. 2016YFA0201603) for financial supports.

Appendix A. Supplementary data

Supplementary material related to this article can be found, in the online version, at doi:<https://doi.org/10.1016/j.toxlet.2018.05.038>.

References

- Akbar, A., Anal, A.K., 2014. Zinc oxide nanoparticles loaded active packaging, a challenge study against *Salmonella typhimurium* and *Staphylococcus aureus* in ready-to-eat poultry meat. *Food Control* 38, 88–95.
- Asri-Rezaei, S., Dalir-Naghadeh, B., Nazarizadeh, A., Noori-Sabzikar, Z., 2017. Comparative study of cardio-protective effects of zinc oxide nanoparticles and zinc sulfate in streptozotocin-induced diabetic rats. *J. Trace Elem. Med. Biol.* 42, 129–141.
- Baek, M., Chung, H.E., Yu, J., Lee, J.-A., Kim, T.-H., Oh, J.-M., Lee, W.-J., Paek, S.-M., Lee, J.K., Jeong, J., Choy, J.-H., Choi, S.J., 2012. Pharmacokinetics, tissue distribution, and excretion of zinc oxide nanoparticles. *Int. J. Nanomed.* 3081–3097.
- Banerjee, A., Qi, J., Gogoi, R., Wong, J., Mitrugotri, S., 2016. Role of nanoparticle size, shape and surface chemistry in oral drug delivery. *J. Controll. Release* 238, 176–185.
- Boholm, M., Arvidsson, R., 2016. A definition frame work for the terms nanomaterial and nanoparticle. *Nanoethics* 10, 25–40.
- Bouwmeester, H., Dekkers, S., Noordam, M.Y., Hagens, W.I., Bulder, A.S., de Heer, C., ten Voorde, S.E.C.G., Wijnhoven, S.W.P., Marvin, H.J.P., Sips, A.J.A.M., 2009. Review of health safety aspects of nanotechnologies in food production. *Regul. Toxicol. Pharmacol.* 53, 52–62.
- Bradley, P.P., Priebe, D.A., Christensen, R.D., Rothstein, G., 1982. Measurement of cutaneous inflammation: estimation of neutrophil content with an enzyme marker. *J. Invest. Dermatol.* 78, 206–209.
- Cho, W., Kang, B.C., Lee, J.K., Jeong, J., Che, J.H., Seok, S.H., 2013. Comparative absorption, distribution, and excretion of titanium dioxide and zinc oxide nanoparticles after repeated oral administration. *Part. Fibre. Toxicol.* 10, 9.
- Contado, C., 2015. Nanomaterials in consumer products: a challenging analytical problem. *Front. Chem.* 3, 48.
- Des Rieux, A., Fievez, V., Garinot, M., Schneider, Y.J., Preat, V., 2006. Nanoparticles as potential oral delivery systems of proteins and vaccines: a mechanistic approach. *J. Control. Release* 116, 1–27.
- Esmaeilou, M., Moharamnejad, M., Hsankhani, R., Tehrani, A.A., Maadi, H., 2013. Toxicity of ZnO nanoparticles in healthy adult mice. *Environ. Toxicol. Pharmacol.* 35, 67–71.
- Espitia, P.J.P., Soares, N.D.F., Coimbra, J.S.D., de Andrade, N.J., Cruz, R.S., Medeiros, E.A.A., 2012. Zinc oxide nanoparticles: synthesis, antimicrobial activity and food packaging applications. *Food Bioprocess. Technol.* 5 (5), 1447–1464.
- Faith, M., Sukumaran, A., Pulimood, A.B., Jacob, M., 2008. How reliable an indicator of inflammation is myeloperoxidase activity? *Clin. Chim. Acta* 396 (1), 23–25.
- FDA (US Food and Drug Administration), 2002. Guidance for Industry and Reviewers: Estimating the Safe Starting Dose in Clinical Trials for Therapeutics in Adult Health Volunteers.
- FDA, CDR (Center for Drug Evaluation and Research), 2005. Guidance for Industry: Estimation of the Maximum Safe Starting Dose in Initial Clinical Trials for Therapeutics in Adult Healthy.
- Gerloff, K., Pereira, D.I.A., Faria, N., Boots, A.W., Kolling, J., Förster, I., Albrecht, C., Powell, J.J., Schins, R.P.F., 2013. Influence of simulated gastrointestinal conditions on particle-induced cytotoxicity and interleukin-8 regulation in differentiated and undifferentiated Caco-2 cells. *Nanotoxicology* 7, 353–366.
- Gulson, B., McCall, M.J., Bowman, D.M., Pinheiro, T., 2015. A review of critical factors for assessing the dermal absorption of metal oxide nanoparticles from sunscreens applied to humans, and a research strategy to address current deficiencies. *Arch. Toxicol.* 89, 1909–1930.
- Hakata, T., Ito, K., Horie, T., 2005. Enhanced absorption of 3-O-methyl glucose following gastrointestinal injury induced by repeated oral administration of 5-FU in mice. *J. Pharmacol. Sci.* 94 (8), 1713–1722.
- Hong, T.K., Tripathy, N., Son, H.J., Ha, K.T., Jeong, H.S., Hahn, Y.B., 2013. A comprehensive in vitro and in vivo study of ZnO nanoparticles toxicity. *J. Mater. Chem. B* 1 (23), 2985–2992.
- Jia, J., Li, F., Zhai, S., Zhou, H., Liu, S., Jiang, G., Yan, B., 2017. Susceptibility of overweight mice to liver injury as a result of the ZnO nanoparticle-enhanced liver deposition of Pb²⁺. *Environ. Sci. Technol.* 51, 1775–1784.
- Kawahara, R., Yasuda, M., Hashimura, H., Amagase, K., Kato, S., Takeuchi, K., 2011. Activation of α 7 nicotinic acetylcholine receptors ameliorates indomethacin-induced small intestinal ulceration in mice. *Euro. J. Pharmacol.* 650, 411–417.
- Kim, M.-K., Lee, J.-A., Jo, M.-R., Choi, S.-J., 2016. Bioavailability of silica, titanium dioxide, and zinc oxide nanoparticles in rats. *J. Nanosci. Nanotechnol.* 16, 6580–6587.
- Lee, C.M., Jeong, H.J., Kim, D.W., Sohn, M.H., Lim, S.T., 2012. The effect of fluorination of zinc oxide nanoparticles on evaluation of their biodistribution after oral administration. *Nanotechnology* 23, 205102.
- Li, C.H., Shen, C.C., Cheng, Y.W., Huang, S.-H., Wu, C.-C., Kao, C.-C., Liao, J.-W., Kang, J.-J., 2012. Organ biodistribution, clearance, and genotoxicity of orally administered zinc oxide nanoparticles in mice. *Nanotoxicology* 6, 746–756.
- Liu, J.-H., Ma, X., Xu, Y., Tang, H., Yang, S.-T., Yang, Y.-F., Kang, D.-D., Wang, H., Liu, Y., 2017. Low toxicity and accumulation of zinc oxide nanoparticles in mice after 270-day consecutive dietary supplementation. *Toxicol. Res.* 6, 134–143.
- Llorens, A., Lloret, E., Picouet, P.A., Trbojevich, R., Fernandez, A., 2012. Metallic-based micro and nanocomposites in food contact materials and active food packaging. *Trends Food Sci. Technol.* 24 (1), 19–29.
- Matula, A., Richter, L., Adamkiewicz, W., Akerstrom, B., Paczesny, J., Holyst, R., 2016. Influence of nanomechanical stress induced by ZnO nanoparticles of different shapes on the viability of cells. *Soft Matter* 12, 4162–4169.
- Memarzadeh, K., Sharili, A.S., Huang, J., Rawlinson, S.C.F., Allaker, R.P., 2015. Nanoparticulate zinc oxide as a coating material for orthopedic and dental implants. *J. Biomed. Mater. Res. A* 103 (3), 981–989.
- Mertz, W., 1981. The essential trace-elements. *Science* 213, 1332–1338.
- Niikura, K., Matsunaga, T., Suzuki, T., Kobayashi, S., Yamaguchi, H., Orba, Y., Kawaguchi, A., Hasegawa, H., Kajino, K., Ninomiya, T., Ijiro, K., Sawa, H., 2013. Gold nanoparticles as a vaccine platform: influence of size and shape on immunological responses in vitro and in vivo. *ACS Nano* 7, 3926–3938.
- Osmond, M.J., McCall, M.J., 2010. Zinc oxide nanoparticles in modern sunscreens: an analysis of potential exposure and hazard. *Nanotoxicology* 4, 15–41.
- Park, H.-S., Kim, S.-J., Lee, T.-J., Kim, G.-Y., Meang, E., Hong, J.-S., Kim, S.-H., Koh, S.-B., Hong, S.-G., Sun, Y.-S., 2014. A 90-day study of sub-chronic oral toxicity of 20 nm positively charged zinc oxide nanoparticles in Sprague Dawley rats. *Inter. J. Nanomed.* 9, 93–107.
- Peters, R., Kramer, E., Oomen, A.G., Rivera, Z.E., Oegema, G., Tromp, P.C., Fokkink, R., Rietveld, A., Marvin, H.J., Weigel, S., Peijnenburg, A.A., Bouwmeester, H., 2012. Presence of nano-sized silica during in vitro digestion of foods containing silica as a food additive. *ACS Nano* 6 (3), 2441–2451.

- Randhawa, P.K., Singh, K., Singh, N., Jaggi, A.S., 2014. A review on chemical-induced inflammatory bowel disease models in rodents. *Korean J. Physiol. Pharmacol.* 18 (4), 279–288.
- Scheers, N., 2013. Regulatory effects of Cu, Zn, and Ca on Fe absorption: the intricate play between nutrient transporters. *Nutrients* 5 (3), 957–970.
- Sharma, V., Singh, P., Pandey, A.K., Dhawan, A., 2012. Induction of oxidative stress, DNA damage and apoptosis in mouse liver after sub-acute oral exposure to zinc oxide nanoparticles. *Mutat. Res. Genet. Toxicol. Environ. Mutagen.* 745, 84–91.
- Srivastav, A.K., Kumar, M., Ansari, N.G., Jain, A.K., Shankar, J., Arjaria, N., Jagdale, P., Singh, D., 2016. A comprehensive toxicity study of zinc oxide nanoparticles versus their bulk in Wistar rats. *Hum. Exper. Toxicol.* 35, 1286–1304.
- Storey, M.L., Greger, J.L., 1987. Iron, zinc and copper interactions: chronic versus acute responses of rats. *J. Nutrition* 117, 1434–1442.
- Swietlicki, J.L.E., Rissler, J., Bengtsson, A., Boman, C., Blomberg, A., Sandström, T., 2012. Experimental determination of the respiratory tract deposition of diesel combustion particles in patients with chronic obstructive pulmonary disease. Part. Fibre Toxicol. 9, 30.
- Umrani, R.D., Paknikar, K.M., 2014. Zinc oxide nanoparticles show antidiabetic activity in streptozotocin-induced types-1 and 2 diabetic rats. *Nanomedicine* 9 (1), 89–104.
- Vance, M.E., Kuiken, T., Vejerano, E.P., McGinnis, S.P., Hochella, Jr.M.F., Rejeski, D., Hull, M.S., 2015. Nanotechnology in the real world: redeveloping the nanomaterial consumer products inventory. *Beilstein J. Nanotechnol.* 6, 1769–1780.
- Wang, B., Feng, W., Wang, M., Wang, T., Gu, Y., Zhu, M., Ouyang, H., Shi, J., Zhang, F., Zhao, Y., Chai, Z., Wang, H., Wang, J., 2008. Acute toxicological impact of nano- and submicro-scaled zinc oxide powder on healthy adult mice. *J. Nanopart. Res.* 10, 263–276.
- Wang, H., Du, L.-J., Song, Z.-M., Chen, X.-X., 2013a. Progress in the characterization and safety evaluation of engineered inorganic nanomaterials in food. *Nanomedicine* 8 (12), 2007–2025.
- Wang, Y., Chen, Z.J., Ba, T., Pu, J., Chen, T., Song, Y.S., Gu, Y.G., Qian, Q., Xu, Y.Y., Xiang, K., Wang, H.F., Jia, G., 2013b. Susceptibility of young and adult rats to the oral toxicity of titanium dioxide nanoparticles. *Small* 9 (9–10), 1742–1752.
- Wang, C., Lu, J., Zhou, L., Li, J., Xu, J., Li, W., Zhang, L., Zhong, X., Wan, T., 2016. Effects of long-term exposure to zinc oxide nanoparticles on development, zinc metabolism and biodistribution of minerals (Zn, Fe, Cu, Mn) in mice. *PLoS One* 11 (10), e0164434.
- Wang, C., Cheng, K., Zhou, L., He, J., Zheng, X., Zhang, L., Zhong, X., Wang, T., 2017. Evaluation of long-term toxicity of oral zinc oxide nanoparticles and zinc sulfate in mice. *Biol. Trace Elem. Res.* 178, 276–282.
- Yamaji, S., Tennant, J., Tandy, S., Williams, M., Singh Srai, S.K., Sharp, P., 2001. Zinc regulates the function and expression of the iron transporters DMT1 and IREG1 in human intestinal Caco-2 cells. *FEBS Lett.* 507 (2), 137–141.
- Yang, S.T., Liu, J.H., Wang, J., Yuan, Y., Cao, A., Wang, H., Liu, Y., Zhao, Y., 2010. Cytotoxicity of zinc oxide nanoparticles: importance of microenvironment. *J. Nanosci. Nanotechnol.* 10, 8638–8645.
- Zhang, H., Chen, B., Jiang, H., Wang, C., Wang, H., Wang, X., 2011. A strategy for ZnO nanorod mediated multi-mode cancer treatment. *Biomaterials* 32, 1906–1914.
- Zhu, P., Weng, Z., Li, X., Liu, X., Wu, S., Yeung, K.W.K., Wang, X., Cui, Z., Yang, X., Chu, P.K., 2016. Biomedical applications of functionalized ZnO nanomaterials: from bio-sensors to bioimaging. *Adv. Mater. Interfaces* 3, 1500494.